Multiphonon Raman scattering in semiconductor nanocrystals: Importance of nonadiabatic transitions

E. P. Pokatilov,* S. N. Klimin,* V. M. Fomin,* and J. T. Devreese[†]
Theoretische Fysica van de Vaste Stoffen, Universiteit Antwerpen (UIA), B-2610 Antwerpen, Belgium

F. W. Wise
Department of Applied Physics, Cornell University, Ithaca, New York 14853

Multiphonon Raman scattering in semiconductor nanocrystals is treated taking into account both adiabatic and nonadiabatic phonon-assisted optical transitions. Because phonons of various symmetries are involved in scattering processes, there is a considerable enhancement of intensities of multiphonon peaks in nanocrystal Raman spectra. Cases of strong and weak band mixing are considered in detail. In the first case, fundamental scattering takes place via internal electron-hole states and is participated in by s and d phonons, while in the second case, when the intensity of the one-phonon Raman peak is strongly influenced by the interaction of an electron and of a hole with interface imperfections (e.g., with trapped charge), p phonons are most active. Calculations of Raman scattering spectra for CdSe and PbS nanocrystals give a good quantitative agreement with recent experimental results.

PACS number(s): 78.30.−j, 63.20.Kr, 61.46.+w, 71.35.−y

I. INTRODUCTION

The symmetry-breaking coupling of vibrational modes to degenerate electronic states described first by Jahn and Teller[1] has been manifested in a wide range of transport and optical phenomena in various electron-vibrational systems. The role of the Jahn-Teller effect in the optical transitions of semiconductor nanocrystals has been recently studied in Refs. 2 and 3 for the strong-confinement regime, when the radius of a nanocrystal R is smaller than the Bohr radius of an exciton in bulk R_{ex}, and in Refs. 4 and 5 for the weak-confinement regime, when $R > R_{ex}$. In the case of a strong confinement, when *all* the states of an exciton, including the ground state, are degenerate due to band mixing, the Jahn-Teller effect substantially influences the phonon-assisted optical transitions already in the framework of the dipole approximation.[2,3] As a result, the optical spectra of nanocrystals with $R < R_{ex}$ can be different from the Franck-Condon progressions typical of the adiabatic systems.

Recently, multiphonon peaks in Raman scattering spectra have been observed in CdSe, CdSe$_x$S$_{1-x}$, and PbS nanocrystals (see, for example, Refs. 6–8). Previously, the theoretical analysis of multiphonon Raman scattering in nanocrystals has been generally based on the adiabatic approximation due to the seminal works of Huang and Rhys[9] and Pekar.[10] However, even taking into account band mixing, the values of the Huang-Rhys factor for nanocrystals of radii $R = 1$ nm to $R = 5$ nm appear to be considerably smaller than unity. This result is at variance with those derived from the experiments cited above. In the present paper, the theoretical treatment is performed involving both adiabatic and nonadiabatic optical transitions. The interaction of phonons with an exciton in a degenerate state leads to *internal nonadiabaticity* of nanocrystals (the Jahn-Teller effect), while the existence of exciton levels separated by an energy comparable with that of the optical phonon results in *external nonadiabaticity* (the pseudo-Jahn-Teller effect). The structural imperfections of the real interface between a nanocrystal and a host medium can also substantially influence the probabilities of phonon-assisted transitions, see, e.g., Ref. 11. Moreover, these imperfections (e.g., trapped charge localized at the interface, as supposed in Refs. 8 and 12) can increase the contribution of nonadiabatic transitions into the scattering probability, as shown below.

In nanostructures, phonon spectra drastically differ from those in bulk materials.[6,13–16] Previously, several models of polar optical phonons and of the electron-phonon interaction have been developed for these structures. The *dielectric continuum* model, which is proposed in Ref. 17 and used for planar,[18–22] cylindrical, and spherical[6,23] structures, exploits only electrostatic boundary conditions. The alternative *hydrodynamic* model (see Refs. 24–27) treats only mechanical boundary conditions. Distinctions between the two models consist in a choice of a complete orthogonal basis for the relative ionic displacement $\mathbf{u}(\mathbf{r})$. It has been shown in Refs. 28 and 29 that physical quantities expressed as a sum over all phonon modes (scattering rates, polaron parameters, etc.) slightly depend on a concrete basis. On the other hand, calculated Raman spectra are sensitive to mechanical boundary conditions. Various improvements of the dielectric continuum model[30,31] are developed in order to obtain better agreement between the macroscopic and microscopic[29,32] description of lattice vibrations and with experimental data on Raman scattering.[33–35] Within the continuum model of optical phonons in spatially confined systems (Refs. 15, 16, and 36–38), both electrostatic and mechanical boundary conditions are imposed on ionic displacement. The *multimode dielectric model* developed by us (see Refs. 39 and 40), in addition, explicitly takes into account a finite number of phonon degrees of freedom in a quantum dot.

65 075316-1

In Sec. II, the set of phonon modes is determined using an effective dielectric function of a nanocrystal in a finite-dimensional basis for the field of ionic displacements. In Sec. III, multiphonon resonant Raman scattering in spherical nanocrystals is considered using the obtained Hamiltonian of the electron-phonon interaction. The obtained analytical and numerical results are discussed and compared with experimental data in Sec. IV.

II. OPTICAL PHONONS IN NANOCRYSTALS

In the present investigation, optical vibrations in spherical quantum dots are considered on the basis of the multimode dielectric model (see Refs. 39 and 40). Polar optical phonons in a semiconductor nanocrystal of radius R embedded into a polar medium can be described within the continuum approach (when $R \gg a_0$, where a_0 is the lattice constant) by the renormalized relative ionic displacement vector

$$\mathbf{w}_k(\mathbf{r}) = \frac{e_k^* \mathbf{u}_k(\mathbf{r})}{V_{0k} \omega_{k,\mathrm{TO}} \sqrt{\varepsilon_0[\varepsilon_k(0) - \varepsilon_k(\infty)]}}, \qquad (1)$$

where $k=1$ for the nanocrystal, $k=2$ for the host medium. For the kth medium, $\mathbf{u}_k(\mathbf{r})$ is the relative ionic displacement, e_k^* is the effective charge of an ion, $\omega_{k,\mathrm{TO}}$ is the frequency of the transverse-optical phonon in the Brillouin-zone center, V_{0k} is the volume of the elementary cell, $\varepsilon_k(\infty)$ and $\varepsilon_k(0)$ are the high-frequency and static dielectric constants, respectively, and ε_0 is the permittivity of vacuum. Dynamics of the nondispersive polar optical phonons is determined by the Born-Huang equation[41] combined with Maxwell equations. In order to analyze the time evolution of $\mathbf{w}_k(\mathbf{r})$ taking into consideration the spatial dispersion, the generalized equation of motion[39] is used,

$$(\omega_{k,\mathrm{TO}}^2 - \omega^2)\mathbf{w}_k(\mathbf{r},\omega) = \omega_{k,\mathrm{TO}}\sqrt{\varepsilon_0[\varepsilon_k(0) - \varepsilon_k(\infty)]}\mathbf{E}_k(\mathbf{r},\omega)$$
$$+ \int_{V_k} \mathbf{T}_k(\mathbf{r} - \mathbf{x})\mathbf{w}_k(\mathbf{x},\omega)d\mathbf{x}. \qquad (2)$$

The right-hand side of Eq. (2) consists of two terms: (i) the long-range force expressed by means of the macroscopic electric field $\mathbf{E}_k(\mathbf{r},\omega)$ induced by the ionic-displacement vector $\mathbf{w}_k(\mathbf{r},\omega)$; (ii) the dispersion term of the short-range force with the spatial-dispersion tensor $\mathbf{T}_k(\mathbf{r})$. The action range of this force can be estimated as a few lattice constants.

The set of equations to determine the polar-optical-phonon dynamics in both the nanocrystal and the host medium consists of Eqs. (2), the electrostatic Maxwell equations, and the equation relating the electric field and the polarization to the electrostatic displacement for each medium. The form of the spatial dispersion tensor $\mathbf{T}_k(\mathbf{r})$ is chosen in such a way that the bulk LO (TO) phonon dispersion ω_{LO} ($\omega_{(\mathrm{TO})}$)$(\mathbf{q})$ be reproduced when the equation of motion (2) is solved in bulk. Further on, anisotropy of the dispersion of bulk phonons is neglected: the bulk-phonon frequencies depend only on the wave number q.

For a nanocrystal, the aforesaid set of equations must be completed by electrostatic and mechanical boundary conditions. In the present work, we choose the following mechanical boundary conditions:[37,39]

$$w_k^\perp = 0 \quad \text{at the interfaces,} \quad k = 1,2. \qquad (3)$$

They lead to a double hybridization of LO and interface modes. For planar multilayer structures, phonon spectra obtained in Ref. 37 when applying Eq. (3) are in excellent agreement with experimental Raman-scattering data.[42]

Owing to the spherical symmetry of a quantum dot, the eigenvectors of phonon modes $\mathbf{g}_{lm}^J(\mathbf{r},\omega)$ correspond to a definite phonon angular momentum l and its z projection m. The index J labels LO- and TO-phonon branches. We seek these eigenvectors as a superposition of orthogonal vector functions $\mathbf{f}_{lms}^J(\mathbf{r})$ that satisfy Eq. (3),

$$\mathbf{g}_{lm}^J(\mathbf{r},\omega) = \sum_s U_{l,s}^J(\omega)\mathbf{f}_{lms}^J(\mathbf{r}). \qquad (4)$$

This basis is subdivided into three subsets describing the following.

(i) LO phonons with definite values of the angular momentum l, its projection m, and of the radial quantum number s,

$$\mathbf{f}_{lms}^{\mathrm{LO}}(\mathbf{r}) = \frac{\sqrt{2/R}}{j_l(b_{l,s})\sqrt{b_{l,s}^2 - l(l+1)}}\left\{ \frac{b_{l,s}}{R}j_l'\left(\frac{b_{l,s}r}{R}\right)\mathbf{Y}_{lm}^{(-1)}(\mathbf{n}) \right.$$
$$\left. + \frac{\sqrt{l(l+1)}}{r}j_l\left(\frac{b_{l,s}r}{R}\right)\mathbf{Y}_{lm}^{(1)}(\mathbf{n}) \right\}, \qquad (5)$$

where $\mathbf{n} = \mathbf{r}/r$, $j_l(x)$ is a spherical Bessel function, $b_{l,s}$ is the sth zero of its derivative $j_l'(x)$, $\mathbf{Y}_{lm}^{(\lambda)}(\mathbf{n})$ ($\lambda = 0, \pm 1$) is a spherical vector of a definite parity.

(ii) TO phonons of the "electric" type,

$$\mathbf{f}_{lms}^{\mathrm{TO},E}(\mathbf{r}) = \frac{\sqrt{2/R}}{a_{l,s}j_{l+1}(a_{l,s})}\left\{ \frac{\sqrt{l(l+1)}}{r}j_l\left(\frac{a_{l,s}r}{R}\right)\mathbf{Y}_{lm}^{(-1)}(\mathbf{n}) \right.$$
$$\left. + \frac{a_{l,s}}{R}\left[j_l'\left(\frac{a_{l,s}r}{R}\right) + \frac{R}{a_{l,s}r}j_l\left(\frac{a_{l,s}r}{R}\right) \right]\mathbf{Y}_{lm}^{(1)}(\mathbf{n}) \right\}, \qquad (6)$$

where $a_{l,s}$ is the sth zero of $j_l(x)$.

(iii) TO phonons of the "magnetic" type,

$$\mathbf{f}_{lms}^{\mathrm{TO},M}(\mathbf{r}) = \frac{\sqrt{2}}{R^{3/2}j_{l+1}(a_{l,s})}j_l\left(\frac{a_{l,s}r}{R}\right)\mathbf{Y}_{lm}^{(0)}(\mathbf{n}). \qquad (7)$$

Dimensionalities of the subsets (5)–(7) are implicitly determined by the inequalities

$$b_{l,s} \lesssim \pi R/a_0 \quad \text{for LO modes,} \qquad (8)$$

$$a_{l,s} \lesssim \pi R/a_0, \quad \text{for TO modes,}$$

which express the fact that the "wavelength" of an optical phonon cannot be smaller than the double lattice constant.

Using the expansion (4) for a joint solution of Eq. (2) and of the Maxwell equations with electrostatic boundary conditions, we arrive at the dispersion equation

$$\frac{l+1}{\varepsilon_1(l,\omega)} + \frac{l}{\varepsilon_2(\omega)} = 0, \tag{9}$$

where $\varepsilon_2(\omega)$ is the dielectric function of the host medium. The function $\varepsilon_1(l,\omega)$ is determined by the formula

$$\frac{1}{\varepsilon_1(l,\omega)} \equiv \frac{1}{\varepsilon_1(\infty)}\left(1 - \sum_s \chi_{l,s} \frac{\omega_{1,\mathrm{LO}}^2(0) - \omega_{1,\mathrm{TO}}^2(0)}{\omega_{1,\mathrm{LO}}^2(Q_{l,s}) - \omega^2}\right), \tag{10}$$

where $Q_{l,s} \equiv b_{l,s}/R$ and the coefficients $\chi_{l,s}$ are

$$\chi_{l,s} = \frac{2l}{b_{l,s}^2 - l(l+1)}. \tag{11}$$

These coefficients possess the property $\Sigma_{s=1}^{\infty}\chi_{l,s} = 1$.

We can interpret $\varepsilon_1(l,\omega)$ as the effective dielectric function of the quantum dot, using a formal analogy of the dispersion equation (9) with that of the dielectric continuum model [cf. Eq. (13) of Ref. 6]. In the "nondispersive" limit, when we set in Eq. (10) $\omega_{1,\mathrm{LO}}(Q_{l,s}) = \omega_{1,\mathrm{LO}}(0)$, the function $\varepsilon_1(l,\omega)$ becomes equal to the "bulk" dielectric function $\varepsilon_1(\omega)$, and Eq. (9) turns into the dispersion equation of the dielectric continuum model.[6] The latter equation provides, in particular, interface phonon frequencies $\omega_{j,\mathrm{I}}(l)$ [$j=1,2$; $\omega_{j,\mathrm{TO}}(0) < \omega_{j,\mathrm{I}}(l) < \omega_{1,\mathrm{LO}}(0)$].

Basis vectors of phonon modes are denoted as $\mathbf{g}_{lm\eta}^J(\mathbf{r})$, where the index η labels the roots of Eq. (9), $\omega_{l,\eta}$, at a definite value of the angular momentum l. Generally speaking, LO-phonon modes cannot be subdivided into bulklike and interface ones. Therefore, they can be considered as hybrids of both these types. The following explicit expression is obtained for the coefficients in Eq. (4):

$$U_{l,s}^{\mathrm{LO}}(\omega_{l,\eta}) = \frac{C_l(\omega_{l,\eta})}{\sqrt{b_{l,s}^2 - l(l+1)}[\omega_{1,\mathrm{LO}}^2(Q_{l,s}) - \omega_{l,\eta}^2]}. \tag{12}$$

The transformation (4) is unitary (see Ref. 39). The normalization constant $C_l(\omega_{l,\eta})$ is then found to be

$$C_l(\omega_{l,\eta}) = \left[\sum_s \frac{1}{[b_{l,s}^2 - l(l+1)][\omega_{1,\mathrm{LO}}^2(Q_{l,s}) - \omega_{l,\eta}^2]^2}\right]^{-1/2}. \tag{13}$$

Finally, the phonon Hamiltonian takes the form

$$\hat{H}_L = \sum_\nu \hbar\omega_\nu\left(\hat{a}_\nu^\dagger\hat{a}_\nu + \frac{1}{2}\right), \tag{14}$$

while the Hamiltonian of the electron-phonon interaction is

$$\hat{H}_{e\text{-}L} = \sum_\nu (\hat{\gamma}_\nu\hat{a}_\nu + \hat{\gamma}_\nu^\dagger\hat{a}_\nu^\dagger), \tag{15}$$

where the set of indexes $\nu = (l,m,\eta)$ labels the obtained LO modes. The amplitudes of the electron-phonon interaction can be explicitly expressed in terms of the unitary-transformation coefficients as follows:

$$\gamma_{lm\eta}(\mathbf{r}) = \frac{2\hbar\omega_{1,\mathrm{LO}}}{\sqrt{R}}\left(\frac{\hbar}{m\omega_{1,\mathrm{LO}}}\right)^{1/2}(\sqrt{2}\pi\alpha_1)^{1/2}Y_{lm}(\mathbf{n})$$

$$\times \sum_s \frac{U_{l,s}(\omega_{l,\eta})}{\sqrt{b_{l,s}^2 - l(l+1)}}\left[\frac{j_l(b_{l,s}r/R)}{j_l(b_{l,s})}\right.$$

$$\left. - \frac{(l+1)\varepsilon_2(\omega_{l,\eta})}{l\varepsilon_1 + (l+1)\varepsilon_2(\omega_{l,\eta})}\left(\frac{r}{R}\right)^l\right], \tag{16}$$

where α_1 is the Fröhlich electron-phonon coupling constant of a nanocrystal. The Hamiltonian of the exciton-phonon interaction has a form similar to Eq. (15) with the replacement of $\hat{\gamma}_\nu$ by the exciton-phonon interaction amplitudes

$$\hat{\beta}_\nu(\mathbf{r}_e,\mathbf{r}_h) \equiv \hat{\gamma}_\nu(\mathbf{r}_e) - \hat{\gamma}_\nu(\mathbf{r}_h). \tag{17}$$

It is worth noting that in CdSe and in PbS, where dispersion of bulk LO phonons is strong (see Refs. 34, 43, and 44), the LO phonon modes as derived from Eq. (9) appear to be hybrids of bulklike and interface vibrations.

III. RAMAN SPECTRA

Within the context of the long-wavelength approximation, the interaction of an electron with an electromagnetic field is described by the operator $\hat{V}(t) = \hat{V}_I e^{-i\Omega_I t} + \hat{V}_S^\dagger e^{i\Omega_S t}$, where the terms $\hat{V}_I$ and $\hat{V}_S^\dagger$ correspond, respectively, to the absorption of a photon with the frequency Ω_I (incoming light) and to the emission of a photon with the frequency Ω_S (scattered light). The interaction amplitude $\hat{V}_{I(S)}$ is proportional to the projection of the electron dipole momentum operator $\hat{\mathbf{d}}$ on the polarization vector $\mathbf{e}^{I(S)}$ of the relevant wave: $\partial^{I(S)} = \mathbf{e}^{I(S)} \cdot \hat{\mathbf{d}}$. From the second-order perturbation theory, the transition probability between an initial $|i\rangle$ and a final $|f\rangle$ state is

$$w_{i\to f} = \frac{2\pi}{\hbar^4}\left|\sum_m \frac{\langle f|\hat{V}_S^\dagger|m\rangle\langle m|\hat{V}_I|i\rangle}{\omega_{mi} - \Omega_I + i\delta}\right|^2$$

$$\times \delta(\omega_{fi} - \Omega_I + \Omega_S), \quad \delta \to +0. \tag{18}$$

Here, ω_{mi} and ω_{fi} are transition frequencies. For phonon-assisted Raman scattering in a semiconductor nanocrystal, $|i\rangle$, $|f\rangle$, and $|m\rangle$ are quantum states of the exciton-phonon system. Both the initial and the final states contain no charge carriers (electrons or holes), so that these states are described by a direct product of a wave function of free phonons with

that of the exciton vacuum. Intermediate states $|m\rangle$ are eigenstates of the Hamiltonian

$$\hat{H} = \hat{H}_{ex} + \hat{H}_{ph} + \hat{H}_{ex\text{-}ph}, \tag{19}$$

where $\hat{H}_{ex}$ is the Hamiltonian of an exciton, $\hat{H}_{ph}$ is the phonon Hamiltonian (14), and $\hat{H}_{ex\text{-}ph}$ is the Hamiltonian of the exciton-phonon interaction.

For definite polarizations of the incoming and the scattered light, the scattering probability is obtained by averaging Eq. (18) over the initial states and by summing over the final ones. Since the phonon Hamiltonian $\hat{H}_L$ is quadratic and the Hamiltonian of the exciton-phonon interaction $\hat{H}_{ex\text{-}L}$ is linear in phonon creation and annihilation operators, an analytical averaging over the equilibrium phonon ensemble can be performed in Eq. (18). As a result, we can express the shape of the Raman spectrum in terms of time-ordered operators averaged over exciton states only,

$$W(\Omega_I, \mathbf{e}_I, \Omega_S, \mathbf{e}_S) = \int_{-\infty}^{\infty} dt\, e^{i(\Omega_S - \Omega_I)t} \int_0^{\infty} d\tau \int_0^{\infty} d\sigma$$

$$\times \exp[-\delta(\tau + \sigma) - i\Omega_I(\tau - \sigma)]$$

$$\times \sum_{\mu_1 \mu_2} \sum_{\mu_1' \mu_2'} (d^I_{\mu_1'} d^S_{\mu_2})^* d^I_{\mu_1} d^S_{\mu_2'}$$

$$\times \exp[i(\tilde{\omega}_{\mu_1}\tau - \tilde{\omega}_{\mu_1'}\sigma)]\langle \mu_1' | \langle \mu_2 | T_{s'} T_s^-$$

$$\times \exp\{\Phi[\hat{\beta}, \hat{\beta}']\} | \mu_1 \rangle | \mu_2' \rangle. \tag{20}$$

Here, $\tilde{\omega}_\mu$ are the frequencies and $d^{I(S)}_\mu \equiv \langle \mu | \hat{d}^{I(S)} | 0 \rangle$ are the dipole-matrix elements for a transition from the exciton vacuum $|0\rangle$ to the eigenstates $|\mu\rangle$ of the Hamiltonian $\hat{H}_{ex}$. The "influence phase" of the phonon subsystem $\Phi[\hat{\beta}, \hat{\beta}']$ is the following operator:

$$\Phi[\hat{\beta}, \hat{\beta}'] = \frac{1}{\hbar^2} \sum_\nu \left\{ \int_0^\tau ds \int_0^\sigma ds' \right.$$

$$\times T^*_{\omega_\nu}(t + s - s')\hat{\beta}'_\nu(s')\hat{\beta}^\dagger_\nu(t + s)$$

$$- \int_0^\tau ds \int_0^s ds'\, T_{\omega_\nu}(s - s')\hat{\beta}_\nu(s)\hat{\beta}^\dagger_\nu(s')$$

$$\left. - \int_0^\sigma ds \int_0^s ds'\, T^*_{\omega_\nu}(s - s')\hat{\beta}'_\nu(s')\hat{\beta}^{\dagger'}_\nu(s) \right\}. \tag{21}$$

In Eqs. (20) and (21), primed (unprimed) exciton-phonon amplitudes are chronologically (antichronologically) ordered operators, which act on primed (unprimed) exciton states. The phonon Green's function

$$T_\omega(t) = \frac{\cosh[\omega(it - \hbar/2k_BT)]}{\sinh(\hbar\omega/2k_BT)} \tag{22}$$

describes the phonon emission and absorption processes.

Because electron-phonon coupling is weak in nanocrystals, such as CdSe, $CdSe_xS_{1-x}$ and PbS, the K-phonon scattering intensity, corresponding to a definite combinatorial frequency $\Sigma_{j=1}^K \omega_{\nu_j}$, can be analyzed to the leading (Kth) order in the electron-phonon coupling constant.[45] The scattering intensity within this *leading-term approach* is then expressed through a squared modulus of the scattering amplitude,

$$F_K^{(\pm)}(\nu_1, \ldots, \nu_K)$$

$$= \sum_{\mu_0 \cdots \mu_K} \frac{d^I_{\mu_0}(d^S_{\mu_K})^*}{\tilde{\omega}_{\mu_0} - \Omega_I + i\tilde{\Gamma}_{\mu_0}}$$

$$\times \prod_{j=1}^K \frac{\langle \mu_j | \hat{\beta}_{\nu_j} | \mu_{j-1} \rangle}{\tilde{\omega}_{\mu_j} - \Omega_I \pm \sum_{k=1}^j (\omega_{\nu_k} \pm i\Gamma_{\nu_k}) + i\tilde{\Gamma}_{\mu_j}}, \tag{23}$$

where $\tilde{\Gamma}_\mu$ is the inverse lifetime of an exciton in the state $|\mu\rangle$, while Γ_ν is the inverse lifetime of a phonon of the mode ν.

The following treatment is related to the regime of strong confinement $R < R_{ex}$, where R_{ex} is the exciton Bohr radius. In this case, the Coulomb electron-hole interaction can be treated as a perturbation, and the concept of the exciton means the same as that of the electron-hole pair.

If one considers states of the electron-hole pair $|\mu_j\rangle$ in Eq. (23) within the model of simple bands, then diagonal matrix elements of amplitudes of the electron-phonon interaction on the wave function of the ground electron-hole state vanish, which suppresses the one-phonon Raman scattering. This suppression can be removed by one of the following mechanisms: (i) the Coulomb electron-hole interaction,[46] (ii) band mixing,[47] (iii) the influence of interface imperfections on the exciton wave functions,[11] (iv) nonadiabatic transitions with the participation of virtual phonons. The latter mechanism exists only beyond the leading-term approach.

Two particular cases are of interest when one of these mechanisms dominates: (i) strong band mixing (CdSe in glass[6,7]), (ii) weak band mixing (PbS in polyvinyl alcohol[8]) when one-phonon transitions are determined mainly by the scattering of an electron and of a hole by the potential due to the imperfections. It is worth recalling that, in the strong-confinement regime, the Coulomb interaction only slightly influences the electron-hole states and the Raman spectra.

For a CdSe nanocrystal, exciton states are analyzed here using the spherical model of the exciton Hamiltonian[48] supplemented by terms describing the electron-hole exchange interaction,[49]

$$\hat{H}_{ex} = \frac{1}{2m_e}\hat{\mathbf{p}}_e^2 + \frac{\gamma_1}{2m_0}\hat{\mathbf{p}}_h^2 - \frac{\gamma_2}{9m_0}(\hat{\mathbf{P}}^{(2)} \cdot \hat{\mathbf{J}}^{(2)}) + V_C(\mathbf{r}_e, \mathbf{r}_h)$$

$$- \frac{2}{3}\epsilon_{exch}a_0^3\delta(\mathbf{r}_e - \mathbf{r}_h)(\hat{\vec{\sigma}} \cdot \hat{\mathbf{J}}), \tag{24}$$

where $\hat{\mathbf{p}}_e$ and $\hat{\mathbf{p}}_h$ ($\mathbf{r}_e$ and $\mathbf{r}_h$) are the electron and hole momenta (coordinate vectors), γ_1 and γ_2 are the Luttinger parameters, m_0 and m_e are the bare-electron mass and the electron-band mass; $\hat{\mathbf{P}}^{(2)}$ and $\hat{\mathbf{J}}^{(2)}$ are irreducible second-rank tensors of the momentum and of the spin-$\frac{3}{2}$ angular momentum of a hole, respectively. The potential of the Coulomb attraction between an electron and a hole in a spherical nanocrystal $V_C(\mathbf{r}_e,\mathbf{r}_h)$ is used from Ref. 39. In Eq. (24), the last term, which is proportional to the scalar product of the electron ($\hat{\vec{\sigma}}$) and hole ($\hat{\mathbf{J}}$) spin operators, describes the electron-hole exchange interaction characterized by the strength constant ϵ_{exch}. In CdSe, this constant is equal to 320 meV.[49] The Coulomb and the exchange interactions between an electron and a hole are treated as perturbations when determining the exciton states. To the zeroth order in these perturbations, the exciton states $|\mu\rangle$ are characterized by a definite electron-spin projection σ and the total angular momentum of a hole F with the z projection M,

$$|\mu\rangle \equiv |1S,\sigma;\mathsf{K},M\rangle = \Psi_{1S}^e(\sigma)\Phi_{\mathsf{K}}^h(M), \qquad (25)$$

where $\mathsf{K} = nS_{3/2}$, $nP_{1/2}$, $nP_{3/2}$, $nP_{5/2}$, etc. The index n labels the solutions of the equations for the radial components of the hole wave function.[47]

In contrast to CdSe, the conduction and valence bands in PbS (Ref. 50) are both nondegenerate. As a result, band mixing in PbS nanocrystals exerts a very small influence on the matrix elements of the exciton-phonon interaction. Note that the exciton-phonon coupling due to this mixing in PbS quantum dots calculated using the four-band envelope-function formalism[8] is over two orders of magnitude smaller than the value of CdSe quantum dots at all radii. Hence, the influence of boundary-structure imperfections on the probabilities of one-phonon optical transitions becomes of paramount importance. This gives us a reason to consider electron-hole states in PbS within the model of simple bands. The influence of interface imperfections is modeled by the potential expanded in spherical harmonics $Y_{lm}(\vartheta,\varphi)$,

$$U_{\text{imp}}(\mathbf{r}) = \sum_{l=1}^{\infty}\sum_{m=-l}^{l} U_{lm}\left(\frac{r}{R}\right)^l Y_{lm}(\vartheta,\varphi), \qquad (26)$$

which obeys the Laplace equation. Exciton quantum states $|\mu_j\rangle$ in Eq. (23) are calculated in the first perturbation approximation on the potential $U_{\text{imp}}(\mathbf{r})$. Calculated scattering intensities are then averaged on the Gaussian distribution of random amplitudes U_{lm} with the variance U_0 as a fitting parameter. Equation (26) describes, in particular, the electrostatic potential induced by *trapped charge*. This charge can build up on the nanocrystals during the steady-state Raman measurements.[8,12]

In Raman-scattering experiments,[6-8] the frequency of the incoming light is chosen to be in resonance with the exciton ground-state energy. Hence, only several lowest levels should be considered when calculating scattering amplitudes (23). Two types of *selection rules* manifest themselves in the phonon-assisted Raman scattering. The first group of selection rules results from the symmetry properties of the *dipole-matrix elements* d_μ^I and $d_{\mu'}^S$: (i) for parallel polarizations

($\mathbf{e}^I \| \mathbf{e}^S$), the projection of the exciton angular momentum is preserved in the scattering process, $M = M'$; (ii) for crossed polarizations ($\mathbf{e}^I \perp \mathbf{e}^S$), $M = M' \pm 1$.

The second group of selection rules is determined by the symmetry properties of matrix elements of the *exciton-phonon interaction* amplitudes $\langle \mu_j|\hat{\beta}_{\nu_j}|\mu_{j-1}\rangle$. Only the following phonons take part in the one-phonon scattering: (i) phonons with $m=0$, in parallel polarizations; (ii) phonons with $m=\pm 1$, in crossed polarizations. The selection rules for the one-phonon Raman scattering in spherical nanocrystals were analyzed in Ref. 16 supposing a nondegenerate parabolic band structure, and the conclusion drawn was that only s phonons (with $l=0$) are active in the dipole scattering processes. This conclusion cannot be applied to nanocrystals with a degenerate valence band, where due to band mixing s phonons and d phonons (with $l=2$) appear to be active in the one-phonon Raman scattering.

In the multiphonon scattering amplitudes of Eq. (23) with the phonon number $K \geq 2$, each matrix element of the exciton-phonon interaction contains at least one *intermediate* quantum state, which can be optically active or inactive. Since in the scattering amplitudes of Eq. (23), the summation is carried out over all intermediate states, phonons of arbitrary angular momenta can participate in multiphonon transitions assisted by more than one phonon. It should be mentioned that the adiabatic approximation allows participation of only s phonons in multiphonon scattering processes.[6]

It is worth noting that the one-phonon Raman scattering assisted by p phonons is *forbidden* in the case when a nanocrystal has inversion symmetry. However, the potential due to imperfections [Eq. (26)] contains both even and odd terms and hence *breaks this symmetry down*. Owing to the breakdown of the inversion symmetry, the p phonons (and other phonons of the odd parity) can be active in the one-phonon Raman scattering.

IV. DISCUSSION OF RESULTS

For the calculation of Raman spectra for CdSe quantum dots, the following values of parameters are used: $\varepsilon_1(\infty) = 6.23$, $\varepsilon_1(0) = 9.56$,[51] the electron band mass $m_e = 0.11m_0$, the bulk energy band gap $E_g = 1.9$ eV,[52] the Luttinger parameters $\gamma_1 = 2.04$, $\gamma_2 = 0.58$,[53] and $\varepsilon_2 = 2.25$.[6]

For PbS quantum dots, we have taken $E_g = 0.307$ eV,[54] $\varepsilon_1(\infty) = 18.5$, $\varepsilon_1(0) = 190$.[55] The energy of the size quantization in the PbS nanocrystals under consideration (with $R \sim 1$ to 2 nm) is considerably larger than the bulk band gap. For such a large energy, the dispersion law of both an electron and a hole is substantially nonparabolic, so that we cannot use the effective-mass approach even for simple bands. In this view, we determine exciton energies from the experimental absorption spectra of Ref. 8. The peak positions observed in Ref. 8 for PbS nanocrystals of radius 1.5 nm correspond to the energies $E_{exc}(1s,1s) \approx 2.06$ eV, $E_{exc}(1p,1p) \approx 3.14$ eV, $E_{exc}(1d,1d) \approx 4.18$ eV. Since the conduction and valence bands in PbS are known to be approximately mirror images of each other, the energies of transitions between the lowest states of an electron and of a
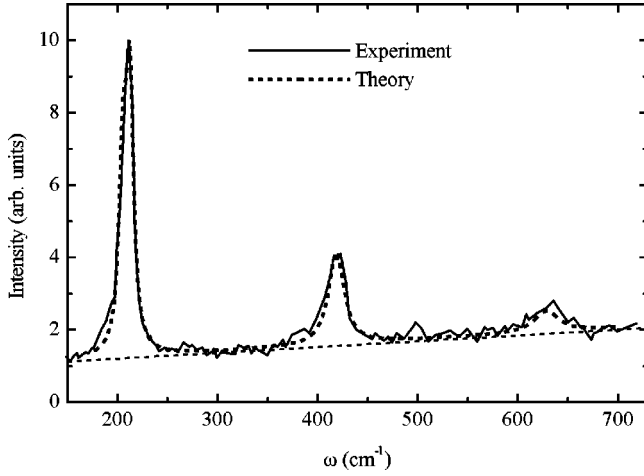
FIG. 1. Multiphonon Raman-scattering spectrum for the ensemble of CdSe nanocrystals with $\langle R \rangle = 2$ nm compared with the experimental data of Ref. 6. The thin dashed line is the luminescence background. The following parameter values are used: $\varepsilon_1(\infty) = 6.23$, $\varepsilon_1(0) = 9.56$ (Ref. 51), $m_e = 0.11 m_0$, $E_g = 1.9$ eV (Ref. 52), $\gamma_1 = 2.04$, $\gamma_2 = 0.58$ (Ref. 53), and $\varepsilon_2 = 2.25$ (Ref. 6).
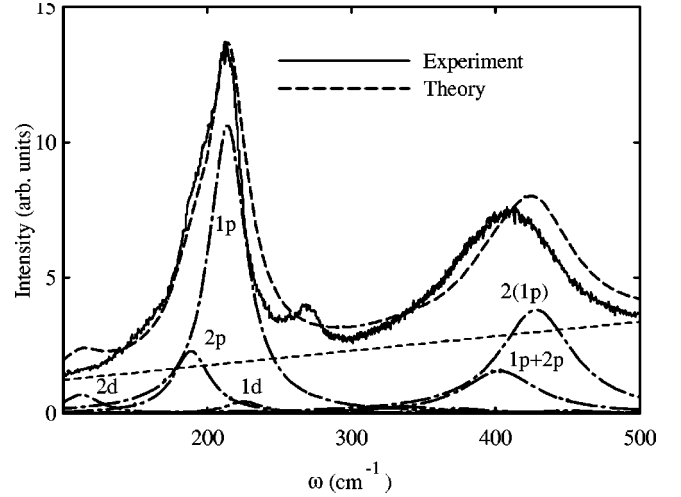

FIG. 2. Calculated Raman-scattering spectrum (the heavy dashed curve) for the ensemble of PbS nanocrystals with $\langle R \rangle = 1.5$ nm. The experimental spectrum of Ref. 8 is shown by the solid line. The following parameter values are used: $E_g = 0.307$ eV (Ref. 54); $\varepsilon_1(\infty) = 18.5$, $\varepsilon_1(0) = 190$ (Ref. 55).

hole can be estimated as $E_{e(h)}(1p) - E_{e(h)}(1s) \approx [E_{exc}(1p,1p) - E_{exc}(1s,1s)]/2 \approx 0.54$ eV, $E_{e(h)}(1d) - E_{e(h)}(1s) \approx [E_{exc}(1d,1d) - E_{exc}(1s,1s)]/2 \approx 1.06$ eV.

The Raman-scattering spectrum, calculated for a Gaussian ensemble of CdSe quantum dots in glass and compared with experimental data of Ref. 6, is shown in Fig. 1. The relative size dispersion $\delta \equiv \sqrt{\langle \Delta R^2 \rangle}/\langle R \rangle$ is taken to be 10% (see Ref. 6). The parameter $\tilde{\Gamma}_\mu \equiv \tilde{\Gamma}$ describing the linewidth of exciton states is taken to be $\tilde{\Gamma} = 0.3 \omega_{1,\text{LO}}$, which is close to values measured in Ref. 56.

The structure of the phonon-assisted Raman-scattering peaks for the spherical CdSe nanocrystals appears to be as follows. According to the selection rules discussed above, only s and d phonons are active in the one-phonon spectrum. In crossed polarizations, transitions assisted by s phonons are forbidden. Hence, the one-phonon spectrum is determined only by d phonons with $m = \pm 1$. In CdSe nanocrystals, the probabilities of transitions are determined mainly by the considerable effect of mixing between bands of heavy and light holes, while the role of interface imperfections is of minor importance. It is worth noting that, as a result of *nonadiabatic transitions* within the state $(1S,1S_{3/2})$, the contribution to scattering intensity due to d phonons is significantly enhanced compared to that calculated[51,57] in the adiabatic approximation. This enhancement is a result of the Jahn-Teller effect. In the multiphonon scattering processes (with $K \geq 2$), the participation of phonons of other types, in particular, p and f phonons, is permitted under the above selection rules. It is also worth noting that transitions assisted by p phonons through excited states $(1S,1P_{3/2})$ and $(1S,1P_{5/2})$ bring a key contribution into the multiphonon scattering probabilities for spherical CdSe quantum dots with typical radii $R \sim 1$ to 4 nm. Recently, in Ref. 46, the multiphonon Raman scattering in spherical semiconductor nanocrystals has been treated within the model[15] for the phonon spectrum and for the

electron-phonon interaction. In Ref. 46, no imperfections and no nonadiabatic effects are taken into account. Relative overtone intensities, calculated in Ref. 46 using the effective-mass approximation for excitonic states, quantitatively differ from the experimental data of Ref. 6. In order to provide a quantitative description of the Raman spectra, in Ref. 46 a correction factor has been introduced. As seen from Fig. 1, our results compare well with those of Ref. 6 without using any correction factors.

The Raman-scattering spectrum obtained for an ensemble of PbS nanocrystals with a relative size dispersion 4% (Ref. 8) is shown in Fig. 2. This spectrum is calculated with $U_0 = 0.036$ eV, which is much less than the typical energy difference between exciton levels. Furthermore, the value $\Gamma_\nu \equiv \Gamma = 15$ cm^{-1} corresponds to the experimentally observed peak broadening, which is attributed to a finite phonon lifetime (see Ref. 8). The fundamental scattering intensity in PbS nanocrystals due to both adiabatic and nonadiabatic transitions is determined by trapped charge and is proportional to U_0^2, while overtone peaks are formed mainly as a result of nonadiabatic transitions through the lowest excited states of an exciton.

The main contribution to both fundamental and overtone bands in PbS quantum dots comes from the exciton-phonon interaction with $1p$ and $2p$ phonons. This contrasts both with the results of the adiabatic approach, which implies a domination of peaks corresponding to s phonons, and with those for CdSe quantum dots, where s and d phonons are active in the fundamental scattering. Peak positions given by the adiabatic theory differ significantly from those of the experimental data.[8]

As a result of considerable LO phonon dispersion in bulk material, the phonon frequencies in PbS quantum dots vary substantially for different modes, i.e., $\omega_{1s} = 235$ cm^{-1}, $\omega_{1p} = 217$ cm^{-1}, $\omega_{2p} = 192$ cm^{-1},

$\omega_{1d} = 229$ cm^{-1}, $\omega_{2d} = 114$ cm^{-1}. Therefore, the phenomena contributing to Raman peaks can be easily identified. In particular, main peaks in both fundamental and overtone bands can be confidently assigned to p phonons. It is evident from Fig. 2, that a satisfactory agreement exists between the calculated Raman spectrum and the experimental results[8] with respect to both ratios between spectral intensities and peak positions.

*Permanent address: Department of Theoretical Physics, State University of Moldova, Strada A. Mateevici 60, MD-2009 Kishinev, Republic of Moldova.

†Also at: Universtiteit Antwerpen (RUCA), Groenenborgerlaan 171, B-2020 Antwerpen, Belgium, and Technische Universiteit Eindhoven, 5600 MB Eindhoven, The Netherlands.

[1] H. A. Jahn and E. Teller, Proc. R. Soc. London, Ser. A **161**, 220 (1937).

[2] V. M. Fomin, E. P. Pokatilov, J. T. Devreese, S. N. Klimin, S. N. Balaban, and V. N. Gladilin, in *Proceedings of the 23rd International Conference on the Physics of Semiconductors*, edited by M. Scheffler and R. Zimmermann (World Scientific, Singapore, 1996), p. 1461.

[3] V. M. Fomin, V. N. Gladilin, J. T. Devreese, E. P. Pokatilov, S. N. Balaban, and S. N. Klimin, Phys. Rev. B **57**, 2415 (1998).

[4] A. V. Fedorov and A. V. Baranov, Zh. Eksp. Teor. Fiz. **110**, 1105 (1996).

[5] A. V. Fedorov, A. V. Baranov, and K. Inoue, Phys. Rev. B **56**, 7491 (1997).

[6] M. C. Klein, F. Hache, D. Ricard, and C. Flytzanis, Phys. Rev. B **42**, 11 123 (1990).

[7] G. Scamarcio, V. Spagnolo, G. Ventruti, M. Lugará, and G. C. Righini, Phys. Rev. B **53**, R10 489 (1996).

[8] T. D. Krauss and F. W. Wise, Phys. Rev. B **55**, 9860 (1997).

[9] K. Huang and A. Rhys, Proc. R. Soc. London, Ser. A **204**, 406 (1950).

[10] S. I. Pekar, Zh. Eksp. Teor. Fiz. **20**, 267 (1950).

[11] M. Nirmal, C. B. Murray, D. J. Norris, and M. G. Bawendi, Z. Phys. D: At., Mol. Clusters **26**, 361 (1993).

[12] T. D. Krauss and F. W. Wise, Phys. Rev. Lett. **79**, 5102 (1997).

[13] R. Englman and R. Ruppin, J. Phys. C **1**, 614 (1968).

[14] H. Richter, Z. P. Wang, and L. Ley, Solid State Commun. **39**, 625 (1981).

[15] E. Roca, C. Trallero-Giner, and M. Cardona, Phys. Rev. B **49**, 13 704 (1994).

[16] M. P. Chamberlain, C. Trallero-Giner, and M. Cardona, Phys. Rev. B **51**, 1680 (1995).

[17] R. Fuchs and K. L. Kliewer, Phys. Rev. **140**, A2076 (1965).

[18] L. Wendler, R. Haupt, F. Bechstedt, H. Rücker, and R. Enderlein, Superlattices Microstruct. **4**, 577 (1983).

[19] R. Lassnig, Phys. Rev. B **30**, 7132 (1984).

[20] N. Sawaki, J. Phys. C **19**, 4965 (1986).

[21] T. Ando and S. Mori, Surf. Sci. **113**, 124 (1982).

[22] R. Enderlein, D. Suisky, and J. Röseler, Phys. Status Solidi B **165**, 9 (1991).

[23] R. Ruppin and R. Englmann, J. Phys. C **1**, 614 (1968).

[24] M. Babiker, J. Phys. C **19**, 683 (1986).

[25] C. Trallero-Giner and F. Comas, Phys. Rev. B **37**, 4583 (1988).

[26] B. K. Ridley, Phys. Rev. B **39**, 5282 (1989).

[27] C. Guillemot and F. Clérot, Phys. Rev. B **44**, 6249 (1991).

[28] K. J. Nash, Phys. Rev. B **46**, 7723 (1992).

[29] H. Rucker, E. Molinari, and P. Lugli, Phys. Rev. B **45**, 6747 (1992).

[30] K. Huang and B. Zhu, Phys. Rev. B **38**, 13 377 (1988).

[31] R. Enderlein, Phys. Rev. B **43**, 14 513 (1991).

[32] K. Huang and B. Zhu, Phys. Rev. B **38**, 2183 (1988).

[33] A. K. Sood, I. Menendez, M. Cardona, and K. P. Ploog, Phys. Rev. Lett. **54**, 2111 (1985); **54**, 2115 (1985).

[34] M. Cardona, Superlattices Microstruct. **5**, 27 (1989).

[35] A. Shields, M. Cardona, and K. Eberl, Phys. Rev. Lett. **72**, 412 (1994).

[36] M. P. Chamberlain, M. Cardona, and B. K. Ridley, Phys. Rev. B **48**, 14 356 (1993).

[37] N. C. Constantinou and B. K. Ridley, Phys. Rev. B **49**, 17 065 (1994).

[38] C. Trallero-Giner, F. Comas, and F. Garcia-Moliner, Phys. Rev. B **50**, 1755 (1994).

[39] S. N. Klimin, E. P. Pokatilov, and V. M. Fomin, Phys. Status Solidi B **190**, 441 (1995).

[40] V. M. Fomin, S. N. Klimin, V. N. Gladilin, and J. T. Devreese, J. Lumin. **87-89**, 330 (2000).

[41] M. Born and K. Huang, *Dynamical Theory of Crystal Lattices* (Clarendon, Oxford, 1968).

[42] M. Haines and G. Scamarcio, in *Phonons in Semiconductor Nanostructures*, Vol. 236 of *NATO Advanced Studies Institute, Series E: Applied Sciences*, edited by J. P. Leburton *et al.* (Kluwer Academic, Holland, 1993), p. 93.

[43] M. M. Elcombe, Proc. R. Soc. London, Ser. A **300**, 210 (1967).

[44] T. D. Krauss, F. W. Wise, and D. B. Tanner, Phys. Rev. Lett. **76**, 1376 (1996).

[45] W. Hayes and R. Loudon, *Scattering of Light by Crystals* (Wiley, New York, 1978).

[46] R. Rodríguez-Suárez, E. Menéndez-Proupin, C. Trallero-Giner, and M. Cardona, Phys. Rev. B **62**, 11 006 (2000).

[47] J. B. Xia, Phys. Rev. B **40**, 8500 (1989).

[48] A. Baldereschi and O. Lipari, Phys. Rev. B **8**, 2697 (1973).

[49] M. Nirmal, D. J. Norris, M. Kuno, M. G. Bawendi, Al. L. Efros, and M. Rosen, Phys. Rev. Lett. **75**, 3728 (1995).

[50] P. J. Lin and L. Kleinman, Phys. Rev. **142**, 478 (1966).

[51] S. Nomura and T. Kobayashi, Phys. Rev. B **45**, 1305 (1992).

[52] *Physics of II-VI and I-VII Compounds, Semimagnetic Semiconductors*, edited by K. H. Hellwege, Landolt-Börnstein, New Series, Group III, Vol. 17, Pt. b (Springer, Berlin, 1982).

[53] D. J. Norris and M. G. Bawendi, Phys. Rev. B **53**, 16 338 (1996).

[54] D. L. Mitchell, E. D. Palik, and J. N. Zemel, in *Proceedings of the 7th International Conference on Physics of Semiconductors*, edited by M. Hulin (Dunod, Paris, 1964), p. 325.

[55] E. Kartheuser, in *Polarons in Ionic Crystals and Polar Semiconductors*, edited by J. T. Devreese (North-Holland, Amsterdam, 1972), p. 728.

[56] D. M. Mittleman, R. W. Schoenlein, J. J. Shiang, V. L. Colvin, A. P. Alivisatos, and C. V. Shank, Phys. Rev. B **49**, 14 435 (1994).

[57] Y. Chen, S. Huang, J. Yu, and Y. Chen, J. Lumin. **60&61**, 786 (1994).